Recovery of ammonium and phosphate from treated urban wastewater by using potassium clinoptilolite impregnated hydrated metal oxides as N-P-K fertilizer

Diana Guaya [a, b*], Mehrez Hermassi [a], Cesar Valderrama [a], Adriana Farran [a], José Luis Cortina [a, c]

[a] Department of Chemical Engineering, Universitat Politècnica de Catalunya-Barcelona Tech (UPC), Barcelona, Spain

[b] Departament of Chemistry, Universidad Técnica Particular de Loja, Loja, Ecuador

[c] Water Technology Center CETaqua, Barcelona, Spain

*Correspondence should be addressed to: Diana Guaya

Email: deguaya@utpl.edu.ec

Abstract

A natural clinoptilolite in its potassium form (KNC) was modified by impregnation of hydrated metal oxides (HMO) of aluminium (III) (KAlC), iron (III) (KFeC) and manganese (IV) (KMnC) for the simultaneous ammonium and phosphate recovery from urban wastewaters. The resulting pH_{pzc} of the HMO on the modified zeolites (7.3±0.3 for KAlC, 6.4±0.4 for KFeC and 6.9±0.3 for KMnC) are suitable for phosphate sorption at pH of treated urban wastewaters (6-8).The sorption capacity for phosphate for KAlC and KFeC zeolites is higher at the lower pH range while for KMnC is higher at the upper pH range. Differences were associated to the differences on the complexing properties of the MOH groups to form outer and inner sphere MOH-phosphate complexes. The maximum phosphate sorption capacity for the three zeolites were 6.8 mg-P/g for KAlC, 7.2 mg-P/g for KFeC and 8.2 mg-P/g for KMnC. Contrary maximum ammonium sorption capacity is kept constant between pH 4 to 9 for the tree zeolites as the main sorption mechanism is the ion-exchange reaction with K^+ ions of the zeolite. The maximum ammonium sorption capacity for the three zeolites ranged from 29 to 33 mg-N/g. These differences on the nature of the sorption processes was traduced in a much faster sorption kinetic for ammonium than for phosphate although for both cases the rate determining

step was ions diffusion on the zeolite particles. Modified zeolites shown high selectivity towards ammonium and phosphate in the presence of the dissolved organic matter as well as other ionic species present in the treated wastewaters. Finally, P fractionation assays of the loaded zeolites confirmed a high phosphate bioavailability if these are applied as phosphate slow release fertilizers in soil applications.

Keywords: potassium clinoptilolite; nutrients recovery; hydrated metal oxides; sorption; NPK fertilizer

1. Introduction

Ammonia nitrogen (NH_4^+-N) and orthophosphate phosphorous (PO_4^{3-} -P) are majors polluting species of aqueous environments [1]. These nutrients are discharged into rivers and lakes from municipal wastewater after being treated, or from run-off of bio-fertilizers applied in farms lands by effect of the rain drainage leading to eutrophication [2]. Currently, phosphate is becoming a major economical concern because its natural deposits are diminishing due to the continuous growth of the world population. Then, urban, industrial and farming wastewaters and sludge streams with phosphorous (P) contents below 1% (w/w) are considered secondary resources of P that need to be mined [3]. There are already a variety of technologies for P recovery at wastewater treatment plants. These technologies differ by the origin of the used resources (wastewater, sludge, sludge liquor, sludge ash), the applied process (precipitation, wet chemical extraction, and thermal treatment) and the potential P-recovery ratio. P could be recovered simultaneously with ammonium from concentrated streams of urban wastewater (e.g. anaerobic digestion side streams) by chemical precipitation of struvite [4]. Few efforts have been directed for the recovery from diluted streams where different techniques for phosphate removal are available [5]. Chemical precipitation and coagulation processes are not cost effective and polymeric ion exchangers are not applicable due to potentially high levels of dissolved and particulate organic matter. Thus, phosphate removal/recovery solutions

have been focused to the use of low-cost adsorbents with high removal efficiency in terms of equilibrium (sorption capacity) and kinetics. Moreover, simultaneous removal of ammonium and phosphate from diluted streams (e.g., treated waste waters from the conventional activated sludge reactors) can be achieved using inorganic adsorbents like natural zeolites [6]. The ammonium removal is favoured by the high cation exchange capacity of natural zeolites [7, 8], however they exhibited poor performance for anions removal (e.g., phosphate) [9]. So, they need a modification stage [10] by incorporating neither cations forming low solubility phosphate minerals (e.g., Ba (II), Ca (II), Mg (II)) [11]; or by incorporating hydrated metal oxides (e.g., Fe, Al, Mn) with complexing properties (inner and outer sphere complexes with phosphate ions). The resulting exhausted sorbents could be used in agriculture and in agronomical applications to improve soil properties in both physical and chemical terms as potential fertilizer as they will provide P and N. The methodology used to modify a granular natural zeolite in sodium form into the Al (III), Fe (II)) and Mn (II) forms and the equilibrium and kinetic properties when used in sorption and desorption cycles was described in previous studies [12, 13]. Therefore, the aim of this work is to evaluate the simultaneous removal of ammonium and phosphate from treated urban wastewater using impregnated aluminium, iron and manganese forms of a powder natural zeolite in its potassium form. The specific objectives proposed are: i) to evaluate the use of powder natural potassium zeolites impregnated with hydrated metal oxides to recover phosphate and ammonium from treated wastewaters and ii) to evaluate the P availability of the loaded N,P,K zeolites for soil quality improvement by using Phosphorous fractioning test of the loaded zeolites.

2. Materials and methods

2.1. Preparation of metal hydrated oxide impregnated zeolites

A natural zeolite (NC) (Zeocem Company from the Slovak Republic) was grounded until particles were below 74 μm. Then, three different samples of 50 g of NC were treated in a 250 mL glass reactor with 0.1 M $AlCl_3$, 0.1 M $FeCl_3$ and 0.1 M $MnCl_2$. After 20 minutes of agitation, the pH of the solutions was adjusted to pH 7±0.5 using 0.1 M KOH (KNC). Then, samples were treated two consecutive times by refluxing in 250 mL of KCl (0.1 M) for 3 h to obtain the aluminium (KAlC), iron (KFeC) and manganese (KMnC) forms of NC zeolite. After treatment, samples were washed until no chloride was detected using an $AgNO_3$ test followed by drying at 80 °C for 24 hours.

2.2. Characterization of metal hydrated oxide impregnated zeolites

A powder X-ray Diffractometer (D8 Advance A25 Bruker) was used for X-ray diffraction (XRD) characterization of KAlC, KFeC, KMnC samples. The phase purity and crystallinity of the powder samples were analysed by X-ray diffraction with λ CuKα radiation (λ= 1.54056 Å)) at a scanning rate time of 19.2 and 57.6 s, steep angle of 0.015° and 2θ in range of 4-60°.

The chemical composition and morphology of the samples were determined by a Field Emission Scanning Electron Microscope (JEOL JSM-7001F) coupled to an Energy Dispersive Spectroscopy system (Oxford Instruments X-Max). The infrared absorption spectra were recorded with a Fourier Transform FTIR 4100 (Jasco) spectrometer in the range of 4000 – 550 cm^{-1}. The nitrogen gas adsorption method was used for the specific surface area determination of KAlC, KFeC, KMnC samples on an automatic sorption analyser (Micrometrics). The tests were replicated at least four times for each sample and the average values are reported.

2.3. Point of cero charge of metal hydrated oxide impregnated zeolites

Samples of impregnated zeolites (KAlC, KFeC, KMnC) were equilibrated in different ionic strengths (25 mL of deionized water; 0.01, 0.05 and 0.1 M NaCl) at 200 rpm and 21±1 °C. The pH drift method was used for point of zero charge (PZC) determination in the range of pH 2 to 11 [14]. Tests were performed in triplicate for each sample and the average values are reported.

2.4. Effect of pH on ammonium and phosphate sorption

Ammonium and phosphate solutions were prepared by dissolving ammonium chloride (NH_4Cl) and sodium phosphate ($NaH_2PO_4.2H_2O$) in deionized water. KAlC, KFeC, KMnC samples (0.1 g) were equilibrated in 25 mL of aqueous solutions containing 25 mg $N\text{-}NH_4^+$/L and 25 mg $P\text{-}PO_4^{3-}$/L (pH adjusted from 2 to 11). The tests were replicated three times for each sample and the average values are reported. Experiments were carried out (in triplicate) using the effluent from secondary treatment at the El Prat wastewater treatment plant (WWTP) (Barcelona – Spain) at its average pH of 7.5. The chemical composition of the treated wastewater used is shown in Table 1.

2.5. Ammonium and phosphate sorption kinetic studies

Weighted amounts of impregnated samples (6 g of KAlC, KFeC, KMnC) were equilibrated in 500 mL of the effluent stream from secondary treatment at the El Prat WWTP (composition shown in Table 1) at pH 7.5±0.5. Experiments were performed at 500 rpm and at room temperature (21±1 °C). Samples (10 mL) were withdrawn at given times for determining the concentrations of ammonium and phosphate ions at the initial and remaining aqueous solution. Tests were performed in triplicate for each sample and the average values are reported. Samples were filtered (0.2 μm) before analysis.

ICP - MS elements											
	Na	Ca	S	K	Mg	Sr	Al	Si	Fe	Ba	
mg/L	246	127	82	36	35	1	0.2	0.03	0.03	0.02	
	Li	B	Ti	V	Cr	Mn	Co	Ni	Cu	Zn	As
µg/L	19	258	6	12	1	3.	2	29	45	61	3
	Se	Rb	Sr	Mo	Sn	Sb	Ba	W	Pb	U	
µg/L	3	16	1091	15	0.3	4	19	3	0.2	2	

Organic and inorganic carbon content					
	NPOC	NT	TOC	TC	IC
mg/L	11.8	296	11	50	42

Major ionic species				
	NH_4^+	PO_4^{3-}	NO_3^-	Cl^-
mg/L	30	14	51	542

Table 1. Chemical composition of the effluent stream from the secondary treatment at the El Prat WWTP (Barcelona, Spain) used for kinetic studies.

Standard methods were used for phosphate and ammonium quantification [15]. The P concentration was analysed by the vanadomolybdophosphoric acid colorimetric method (4500-P C) and N was determined by ammonia-selective electrode method (4500-NH3 D). It was also used a Thermo Scientific Ionic Chromatograph (Dionex ICS-1100 and ICS-1000) for ions quantification. The non-purgeable organic carbon (NPOC), total carbon (TC), total organic carbon (TOC), inorganic carbon (IC) and total nitrogen (NT) were determined in a total organic carbon analyser (Shimadzu, TOC-V_{CPH}). Finally, an elemental analysis including traces existent in the treated wastewater effluent was performed by Inductively Coupled Plasma Mass Spectrometry (ICP-MS) at CSIC, Barcelona - Spain.

2.6. Sequential chemical fractionation of phosphorous on loaded zeolites samples

The modified zeolites were loaded in a solution containing 500 mg/L of ammonium and phosphate ions, and then they were filtered and dried for the sequential chemical fractionation of phosphorus by

an adaptation of the Hedley method [16]. The sequential P extraction was performed to classify and quantify P fractions of the loaded modified zeolites. Samples (0.5 g of KAlC, KFeC, KMnC) were added to 20 mL of each extracting solution 0.5 M $NaHCO_3$ (pH 8.5), 0.1 M NaOH and 1.0 M HCl. The tubes were shaken for 16 h and then the suspensions were centrifuged at 8000 rpm for 10 min and filtered (0.45 µm). The supernatant was collected and stored until analysis and the remaining soil was re-suspended for succeeding extractions. An aliquot of the $NaHCO_3$ and NaOH extracts was acidified to precipitate extracted organic matter and the supernatant was analysed for inorganic phosphorus (P_i). Another aliquot of the extracts was digested with acidified ammonium persulfate in an autoclave at 120 kPa and 121 °C (60 min and 90 min for the $NaHCO_3$ and the NaOH extract, respectively) to convert organic into inorganic form; total phosphorus (P_t) in the digest was analysed spectrophotometrically. The organic phosphorus (P_o) in $NaHCO_3$ and NaOH extracts was calculated as the difference between P_t and P_i of the respective extracts. Residual P in soil samples was determined after digestion with H_2SO_4/H_2O_2. The P concentration in all extracts and digestion solutions was determined spectrophotometrically at 882 nm [17]. Among the P pools, $NaHCO_3$-P is considered to be labile whereas NaOH-P, HCl-P and residual P are referred to as non-labile [18, 19].

2.7. Kinetic data treatment of ammonium and phosphorous removal

Zeolites are characterized by a highly regular porous structure with cavities and interconnected channels that can be penetrated by specific ions while others are excluded. Hence, two different types of pores exist: micropores in the crystals and macropores in the binding network. The Homogeneous Diffusion Model (HDM) and the Shell Progressive Model (SPM) [20] were selected to describe phosphate and ammonium removal by MHO impregnated potassium zeolites. In the HDM model the zeolite is considered as a quasi-homogeneous media and the sorption diffusion rate controlling step on the spherical particles leads to:

i) if particle diffusion D_p ($m^2\ s^{-1}$) controls the sorption rate as described by Eq. 1:

$$-\ln(1-X(t)^2) = \frac{2\,\pi^2 D_p}{r^2}\,t \qquad (1)$$

ii) if liquid film diffusion D_f ($m^2\ s^{-1}$) controls the sorption rate is described by Eq. 2:

$$-\ln\big(1-X(t)\big) = \frac{D_f C}{h\,r\,C_z}\,t \qquad (2)$$

Where X(t) is the fractional attainment of sorption equilibrium (q_t/q_e) on the zeolite phase at time t, C_s and C_r (mg kg^{-1}) are the concentrations of solute in solution and in the zeolite, respectively; r is the average radius of zeolite particles ($4x10^{-4}$ m), t is the contact time (min or s); and h is the thickness of film around the zeolite particle ($1x10^{-5}$ m for poorly stirred solution) [21]. In the SPM, as the porosity of the zeolite is considered small and thus practically impervious to the fluid reactant and the sorption process is described by a concentration profile of the solution containing phosphate and ammonium ions advancing into a spherical zeolite particle partially saturated [20]. The sorption rate controlling steps on the zeolite particles leads to:

(a) if it is controlled by the fluid film K_F ($m\ s^{-1}$) described by Eq. 3:

$$X(t) = \frac{3C_{Ao}K_F}{a_s r C_{so}}\,t \qquad (3)$$

(b) if it is controlled by the diffusion though the particle sorption layer D_p ($m^2\ s^{-1}$), described by Eq. 4:

$$\big[3-3(1-X(t))^{2/3}-2X(t)\big] = \frac{6D_pC_{Ao}}{a_s r^2 C_{so}}\,t \qquad (4)$$

(c) if it is controlled by the chemical reaction k_s ($m^2\ s^{-1}$), described by Eq. 5:

$$\big[1-(1-X(t))^{1/3}\big] = \frac{k_s C_{Ao}}{r}\,t \qquad (5)$$

Where C_{Ao} and C_{So} are the concentration of solute in bulk solution and at the zeolite unreacted core, respectively (mg L^{-1}) and a_s is the stoichiometric coefficient.

All experimental data were treated graphically and compared to all fractional attainment of equilibrium functions (F(X) = f (t)) defined previously for both models HDM and SPM.

3. Results and discussion

3.1. Zeolites characterization

The natural zeolite was mainly identified as clinoptilolite and traces of cristobalite and mordenite were identified through XDR analysis (Figure 1).

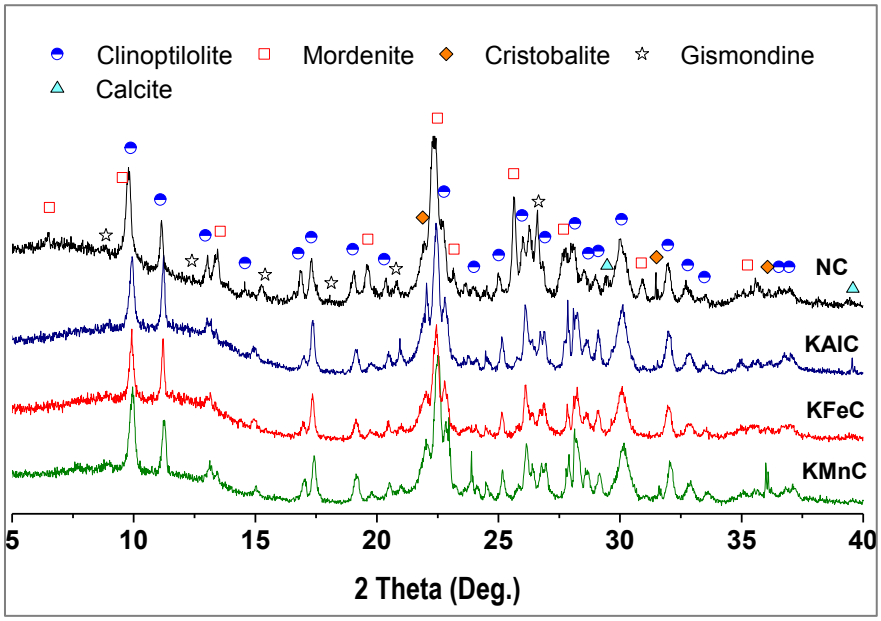

Figure 1. X-ray diffractograms of NC, KAlC, KFeC and KMnC.

The natural zeolite not exhibited a highly pure and crystalline nature. It was not observed any significant attenuation of the peak intensity of the modified forms of NC zeolite revealing the absence of changes on the structure of the raw NC after the modification with aluminium, iron and manganese. The absence of new mineralogical phases and also of significant shift in peaks position of the modified samples suggested that K^{+} and remaining non-precipitated Al^{3+}, Fe^{3+} and Mn^{2+} ions are not modifying the raw material structure (NC) [22]. The chemical composition of the natural and

modified zeolites is collected in Table 2. The three modified materials revealed a reduction in the sodium, magnesium and calcium content that was accompanied by the slight increase of potassium percentage, in comparison with the natural zeolite. Clinoptilolite plate-like morphology that was characterized by networks of crystal clusters with cavities and entries to the channels inside the framework is shown in Figure S1a-d (supplementary information) [23]. The surfaces of the modified zeolites were covered of small particles and crystals uniformly distributed which is in accordance with previous reports [24]. The FTIR analysis of the parent zeolite NC and its aluminium, iron and manganese forms are shown in Figure S2 (supplementary information). A slight variation in the intensity of the peaks in the range from 3700 cm^{-1} to 2951 cm^{-1}, at 1630 cm^{-1} and at 1012 cm^{-1} was observed in the three modified zeolites in comparison to the parent zeolite. The range of bands from 3700 cm^{-1} to 2951 cm^{-1} was assigned to the hydroxyl region of zeolitic structure: SiO–H groups, AlO–H groups, bridging hydroxyls, and H-bonded species [25]. The decrease of the intensity of these bridging Si(OH)Al groups was attributed to the substitution of protons for positively charged M: Al (III), Fe (III) and Mn (II) species. Then, these changes could be attributed to the formation of Al^{3+}–OH, Fe^{3+}–OH and Mn^{2+}–OH hydroxyl sites, which generated the variation of intensity in the band of deformation vibration of water band at ~1630 cm^{-1} [26]. The change of intensity in the peak at ~1012 cm^{-1} also suggested the structural changes promoted by the incorporation of transition metals into zeolite structure [27]. Additionally, the appearance of new peaks below peak at 1558 cm^{-1} when the Al^{3+}, Fe^{3+} and Mn^{2+} are exchanged, can be associated to the amount of Brønsted and Lewis acid sites variation [22].

Sample	O	Na	Mg	Al	Si	K	Ca	Fe	Mn
NC	57.9±3	0.3±0.1	0.4±0.1	5.3±0.4	29.7±2	2.9±1	1.9±0.3	1.6±0.2	-
KAlC	46.6±1	<loq*	<loq*	5.6±1	14.7±2	3.4±1	<loq*	<loq*	-
KFeC	42.4±3	<loq*	<loq*	2.7±0.3	15.6±3	3.4±1	<loq*	8.9±1	-
KMnC	47.8±3	<loq*	<loq*	3.8±1	21.9±5	3.4±1	<loq*	<loq*	1.6±0.2

*loq: limit of quantification

Table 2. Relative atomic percentages measured by EDX of natural and modified zeolites.

The acid–base characterization measured a pH_{pzc} of 5.2±0.4 for parent zeolite in comparison to modified zeolites pH_{pzc} (7.3±0.4 for KAlC, 6.4±0.4 for KFeC and 6.9±0.4 for KMnC). The pH_{pzc} provides information about the sorbent surface charge, and then a slight increase of the point of zero charge after modification can be attributed to the surface nature of impregnated HMO. It was reported in previous studies that metal oxides developed a surface charge with water contact [28] and its interfacial behaviour is promoted by the dissociation of functional groups on the active sites of the sorbent [29]. The values of pH_{pzc} determined for modified zeolites are in agreement with those reported for an aluminium oxide γ-AlOOH (HAO) with 7.26 [30], for an iron oxide supported on a modified zeolite with 6.23 [31], and for manganese oxide Mn_2O_3 with 6.7 [32]. The development of negative charges is obtained for solutions with pH above pH_{pzc}, while pH below pH_{pzc} characterise positive charges development. The pH_{pzc} in modified zeolites KAlC, KFeC and KMnC revealed the existence of positive charges near below the common pH of real municipal wastewater (pH ~7), favouring the adsorption of orthophosphate anions [33].

3.2. Ammonium and phosphate sorption as function of pH

The removal of ammonium can be described by an ion exchange reaction with potassium ions as is described by Eq. 6.

$Z\text{-}K^+ + NH_4^+ \leftrightarrow K^+ + Z\text{-}NH_4^+$ (6)

where Z^- represents the ionogenic groups of the zeolite structure.

The selectivity of the exchange process is considered mainly affected by the ionic charge and ionic radius. Although the Stokes hydration ionic radius for both ions is similar (130 nm) the differences in selectivity for the exchange of K^+/NH_4^+ is enough to assure a high removal efficiency for ammonium [34].

The influence of pH on ammonium sorption capacity of the modified forms of zeolite KAlC, KFeC and KMnC is plot in Figure 2. A similar behaviour of the ammonium sorption capacity as function of pH was obtained for NC. The repulsion of ammonium ions with the positive charges existing on the surface of the modified sorbents was observed below the pH_{pzc} in the acid range from pH 2 to pH 4. Then, the maximum values of ammonium sorption capacity were reached between pH 4 to 7 which is near below the pH_{pzc} of the sorbents. However, above pH_{pzc} it was observed a progressive reduction of ammonium sorption capacity since at pH 7 starts the decrease of the NH_4^+ ion concentration and the conversion to the NH_3 form [35].

The aluminium and iron hydrated oxide forms revealed similar pH dependence behaviour on phosphate sorption. The highest value of sorption capacity was reached at pH 3, which is below the pH_{pzc} of these sorbents; so the presence of positive charges favoured the anion sorption. However, the reduction of phosphate capacity at pH 2 seems to be connected to the conversion of charged phosphate species (e.g. $H_2PO_4^-$) to non-charge H_3PO_4. In the range from pH 4 to 11, near and above the pH_{pzc} of these sorbents, the decrease of phosphate sorption was attributed to the existence of negative surface charged species. Moreover, for the manganese zeolite, low values of phosphate sorption in the pH range from 2 to 6 were measured, and then suddenly increased from pH 7 to pH 10. The phosphate oxyanions ($H_2PO_4^-$ - HPO_4^{2-}) sorption ocurred through chemical reaction via

complexes formation with HMO functional groups (≅MOH). According to these removal patterns observed, the phosphate sorption in the expected pH range (Eq. 7 to 9) could be explained as follow:

- Formation of outer-sphere complexes with $\cong MOH_2^+$ surface groups, described by Eq. 7:

$$\cong MOH_2^+X^- + (H_2PO_4^-/HPO_4^{2-}) \leftrightarrow \cong MOH_2^+(H_2PO_4^-/HPO_4^{2-}) + X^- \quad (7)$$

- Formation of inner-sphere complexes with ≅MOH surface groups, described by Eq. 8:

$$\cong MOH + H_2PO_4^-/HPO_4^{2-} \leftrightarrow \cong MH_2PO_4^-/HPO_4^{2-} + OH^- \quad (8)$$

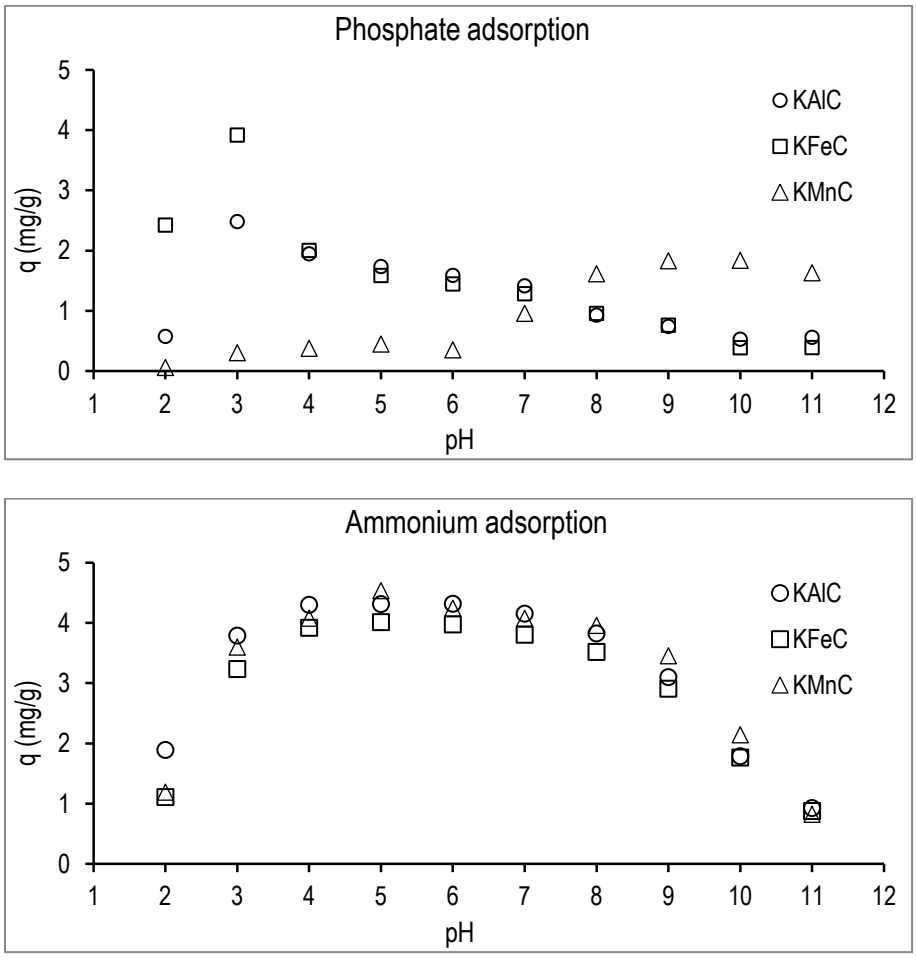

Figure 2. Effect of pH on the removal of ammonium and phosphate on modified zeolites KAlC, KFeC and KMnC.

3.3. Kinetic of phosphate and ammonium sorption

Kinetic sorption data for ammonium and phosphate for KAlC, KFeC and KMnC zeolites are shown in Figure 3. The ammonium sorption rates are comparable for the three modified zeolites which reached the equilibrium in only 15 minutes; whereas the phosphate sorption rates were lower and more than 60 minutes were needed to reach equilibrium. It can suggest that the ion exchange reaction between NH_4^+/K^+ (Eq. 6) occurred faster than complexation reactions of phosphate ions (Eq. 8 and 9). It can be explained due to the better access of the ammonium cations to the negative sites in comparison to the access of the surface hydroxide groups on the solid surface.

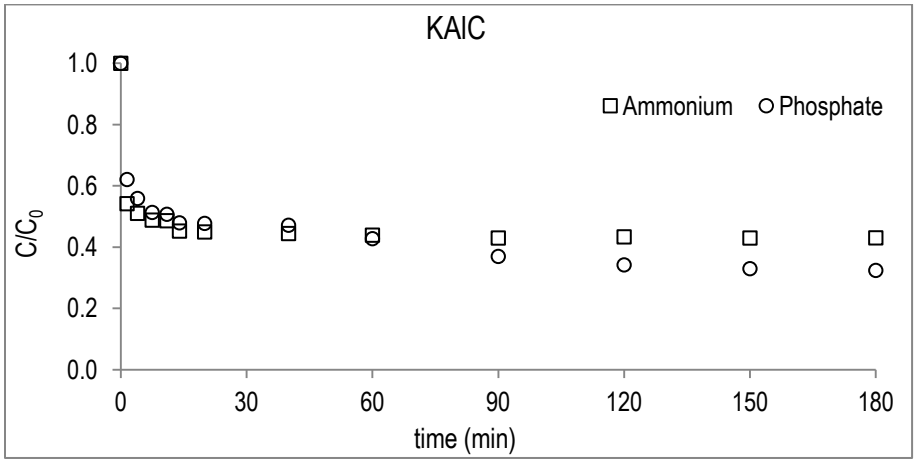

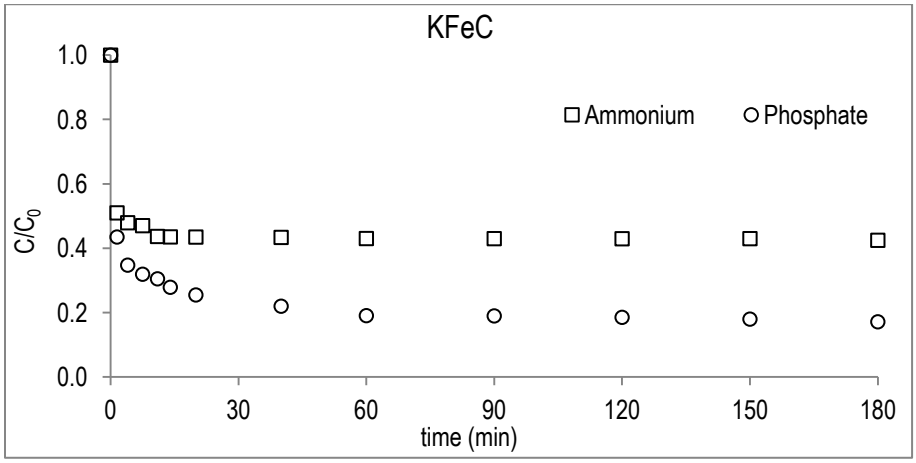

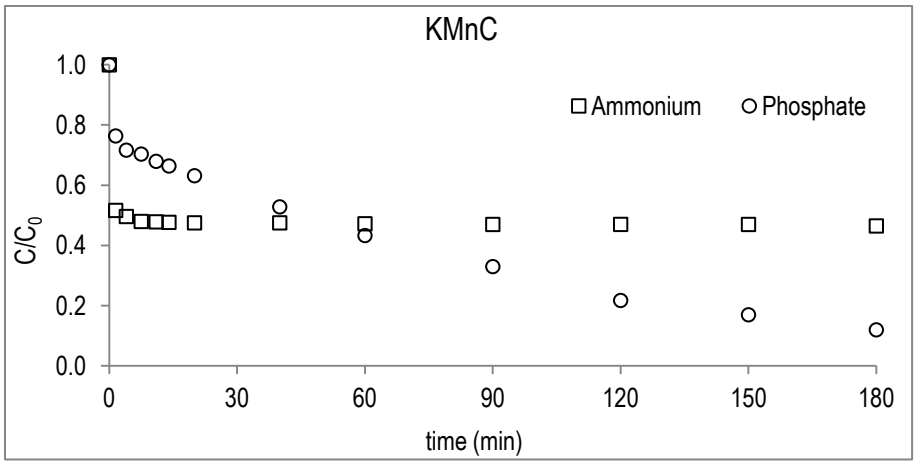

Figure 3. Ammonium and phosphate kinetic adsorption curves of KAlC, KFeC and KMnC zeolites in treated wastewater effluent sample.

The KMnC zeolite exhibited a lower phosphate sorption rate than KAlC and KFeC zeolites; and indeed the sorption capacity showed an increase of removal from 57% up to 78% (50% relative increase) after 30 minutes. This behaviour indicates that the main sorption mechanism involved in phosphate uptake is precipitation.

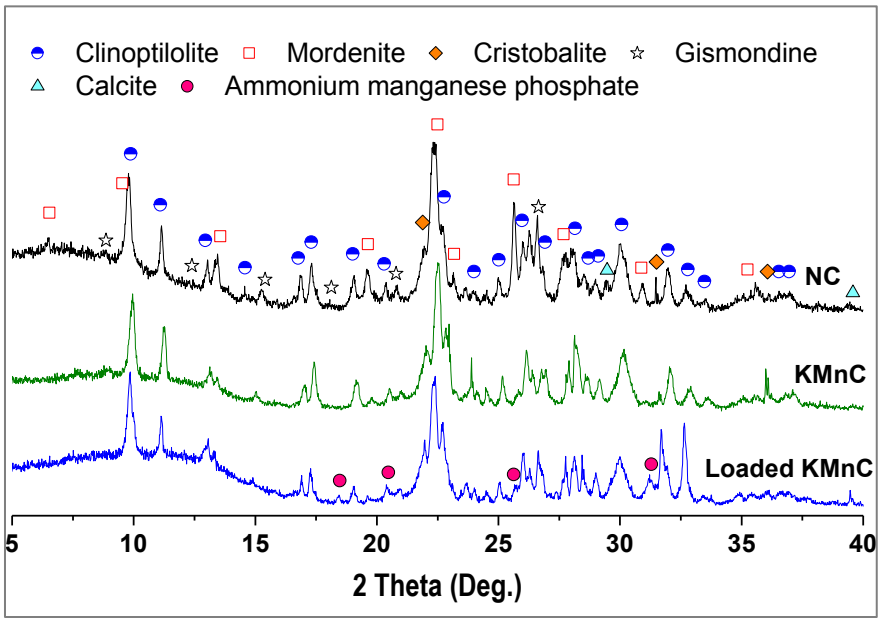

Figure 4. X-ray diffractograms of NC, KMnC and loaded KMnC. (ammonium manganese phosphate ($NH_4MnPO_4 \cdot H_2O$)).

The chemical precipitation of a new crystalline phase was revealed and identified as ammonium manganese hydrogen phosphate ($NH_4MnPO_4 \cdot H_2O$) through the XRD patterns of the loaded modified potassium manganese clinoptilolite KMnC as shown in Figure 4. In the case of KAlC and KFeC neither phosphate-Al nor phosphate-Fe phase was identified after sorption tests.

Analysis of the fractional equilibrium attainment functions (X versus t) by using both HDM and SPM models (Eq. 1-5) indicated that sorption rate control of ammonium and phosphate ions is particle diffusion. A first stage of NH_4^+ and $HPO_4^{2-}/H_2PO_4^-$ diffusion from the solution to the external surface of zeolite is followed by a sorption stage along the zeolite internal surface. The linear regression analyses of the rate control equations for ammonium and phosphate sorption onto modified zeolites are summarized in Table 3. The R^2 values are closer to 1 for D_p than D_f attributing to particle diffusion as the rate-limiting step for both ions. The HPDM and SPM models provided a good description of the kinetic ammonium and phosphate experimental data as can be seen in Figure S3 (supplementary information).

		HPDM				SPM					
		$-\ln(1-X^2)$		$-\ln(1-X)$		X		$[3-3(1-X)^{2/3}-2X]$		$[1-(1-X)^{1/3}]$	
		R^2	D_f ($m^2 \cdot s^{-1}$)	R^2	D_p ($m^2 \cdot s^{-1}$)	R^2	K_F ($m \cdot s^{-1}$)	R^2	D_p ($m^2 \cdot s^{-1}$)	R^2	k_s ($m \cdot s^{-1}$)
KFeC	Phosphate	0.97	$1.1\ 10^{-13}$	0.86	$1.1\ 10^{-8}$	0.83	$2.9\ 10^{-10}$	0.97	$6.8\ 10^{-14}$	0.84	$4.6\ 10^{-10}$
KMnC		0.98	$2.2\ 10^{-14}$	0.91	$1.4\ 10^{-8}$	0.94	$7.4\ 10^{-10}$	0.99	$2.2\ 10^{-14}$	0.93	$2.1\ 10^{-10}$
KAlC		0.99	$1.1\ 10^{-13}$	0.93	$2.9\ 10^{-8}$	0.72	$8.3\ 10^{-9}$	0.98	$5.0\ 10^{-14}$	0.84	4.910^{-10}
KFeC	Ammonium	0.99	$1.1\ 10^{-12}$	0.92	$3.7\ 10^{-8}$	0.79	$3.2\ 10^{-9}$	0.98	$4.6\ 10^{-13}$	0.87	$7.9\ 10^{-10}$
KMnC		0.98	$5.7\ 10^{-13}$	0.86	$2.1\ 10^{-8}$	0.79	$1.2\ 10^{-10}$	0.97	$2.6\ 10^{-13}$	0.86	$1.4\ 10^{-10}$
KAlC		0.99	$2.6\ 10^{-13}$	0.89	$1.4\ 10^{-8}$	0.75	$2.3\ 10^{-9}$	0.99	$2.1\ 10^{-13}$	0.87	$3.5\ 10^{-10}$

Table 3. Kinetic parameters for ammonium and phosphate removal by modified zeolites using both HPDM and SPM models.

The effective diffusion coefficients in the range of 10^{-14}-10^{-12} m^2/s for both ions are common with chemisorption systems [36] and similar to those reported with powder synthetic zeolites used for ammonium or phosphate removal. The effective diffusion coefficients for ammonium ions are higher than for phosphate ions due to the different internal structure of the sites responsible for the sorption mechanism, ion-exchange for ammonium, and surface complexation for phosphate ions. Onyango et al. [37] reported effective diffusion coefficients in the order of 10^{-15} to 10^{-14} m^2/s for phosphate removal with synthetic zeolites impregnated with Al (III) hydrated oxides.

Sorption selectivity of ammonium and phosphate in front of sodium, calcium, magnesium, chloride, sulphate and nitrate, major ions present in the treated wastewaters, for the impregnated zeolites is plot in Figure 5. For the three zeolites, the concentration ratio (C/C_0) decreases with time. A different trend was observed for K^+ as the concentration in solution increased due to the exchange with Na^+/Mg^{2+} and also for Ca^{2+} as expected according to Eq. 6. The selectivity order of K-zeolites for monovalent cations is as follows, $NH_4^+ > K^+ > Na^+$, while for the divalent cations the amount of exchanged cations leads to an equilibrium by about 30 min. The exchanged amount of Ca^{2+} and Mg^{2+} are higher compared to that of monovalent cations, especially for KAlC and KFeC zeolites. The three impregnated potassium zeolites were very selective for the simultaneous ammonium and phosphate sorption as it was reported for aluminium and iron impregnated zeolites [12, 13], taking into account the ions present in real wastewaters that were not sorbed. It should be pointing out that the KMnC zeolite showed the highest selectivity.

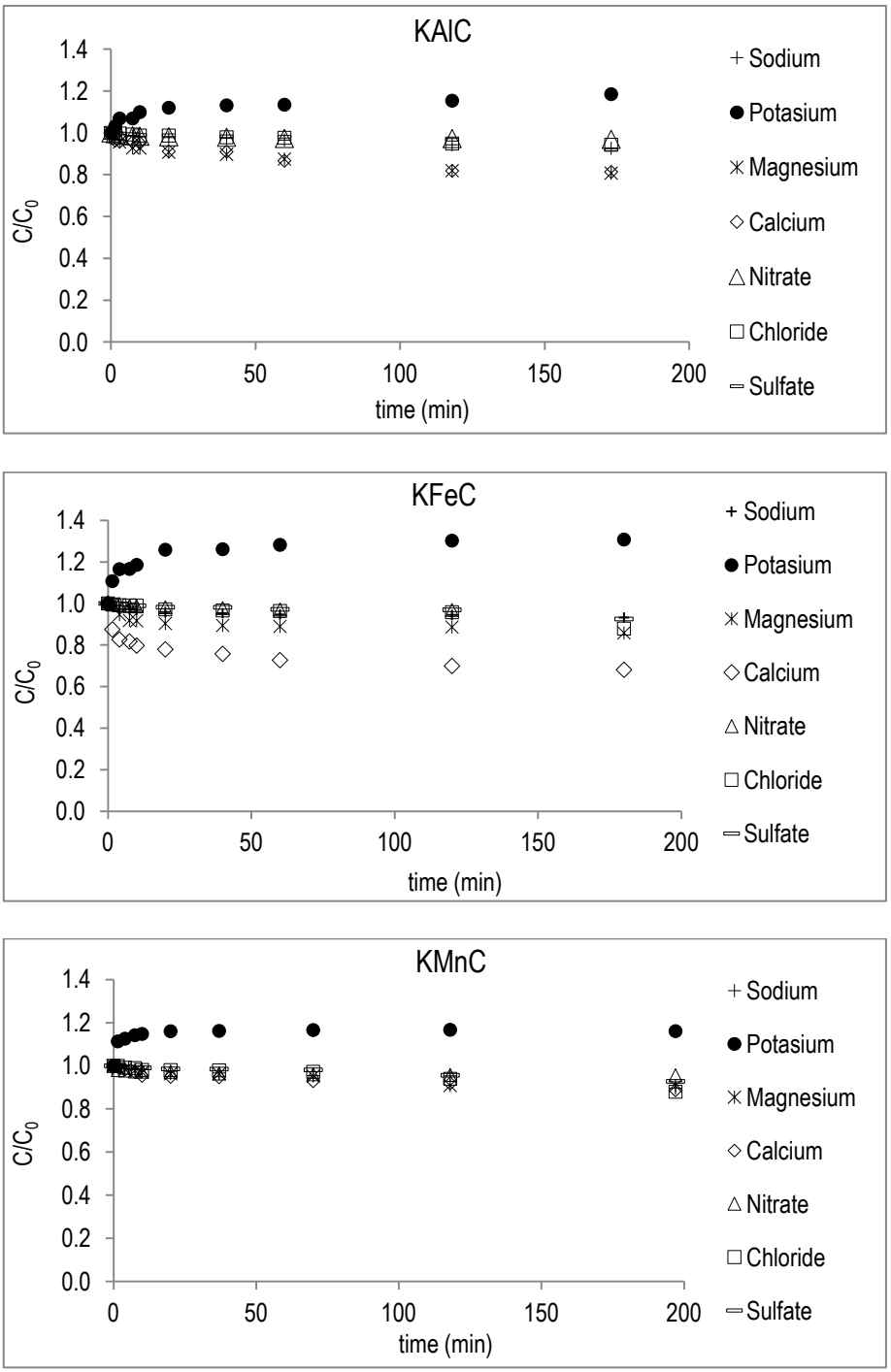

Figure 5. Sorption of cations and anions present in treated wastewater effluent for ammonium and phosphate sorption on modified zeolites KAlC, KFeC and KMnC.

The organic matter sorption of the zeolites, as a function of their major components, purgeable organic carbon (NPOC), total organic carbon (TOC), and total carbon (TC) is listed in Table 4.

Sorption values were below 0.3 mg/g indicating a limited sorption capacity of the zeolites for organic matter under working range evaluated (e.g., 20 mgTOC/L for the test solutions). Then a low influence of the dissolved organic matter on ammonium and phosphate removal can be expected for the three impregnated zeolites. This behaviour is in accordance with previous reports about inorganic sorbents used for nutrients removal which were not affected by low concentration of organic matter [38]. However influence of the organic matter was observed when high organic content is present in contaminated waters [6, 39].

Sample \ Ion	Adsorption capacity ($mg \cdot g^{-1}$)											
	Na^+	K^+	Mg^{2+}	Ca^{2+}	NO_3^+	Cl^-	SO_4^{2-}	NPOC	NT	TOC	TC	IC
KAlC	1.6	-1.8*	0.9	1.4	0.1	2.5	1.8	0.1	1.6	0.3	0.1	0.2
KFeC	1.4	-3.0*	0.7	2.8	0.3	5.3	1.6	0.1	2.1	0.1	<l.d	0.1
KMnC	2.2	-1.3*	0.4	0.9	0.2	5.2	1.6	0.1	2.0	0.1	<l.d	<l.d

<l.d: values below the limit of detection
*Negative values means desorption of the ion from the zeolite to the solution

Table 4. Adsorption capacity of species present in treated wastewater samples.

3.4. Evaluation of phosphate bioavailability of loaded impregnated zeolites by sequential chemical phosphorus fractionation

Sequential chemical phosphorous fractionation data collected in Table 5 revealed that the major fraction of P after the leaching steps is associated with inorganic form (P_i). This in accordance with the fact that the real treated wastewater effluent sample used contained mostly the inorganic form of phosphorus because of WWTP treatment stages involving physical and chemical process.

The major P fraction was found to be the biological active HCO_3^- fraction that was around 35 – 39% of total P. The second P fraction was found to be the NaOH fraction which is associated with formation Fe-Al-Mn hydroxide minerals with 28 – 36% of total P. The third P fraction was found to be

the HCl extractable fractions associated with Ca-P and Mg-P between 26 – 28% of total P. The minor P fraction was the H_2SO_4/H_2O_2 fraction accounting 2 – 3% of total P.

Treatment / Sample		HCO_3			NaOH			HCl			H_2SO_4/H_2O_2
	q	P_i	P_o	P_t	P_i	P_o	P_t	P_i	P_o	P_t	P_r
	$mg.g^{-1}$	$mg.g^{-1}$									
KAlC	6,3	1,7	0,3	2,0	1,6	0,3	1,9	1,3	0,3	1,5	0,2
KFeC	5,6	1,7	0,2	1,8	1,5	0,3	1,9	1,2	0,2	1,3	0,1
KMnC	9,6	2,0	0,3	2,3	1,4	0,3	1,7	1,5	0,20	1,7	0,2

Table 5. Sequential phosphorus fractionation of the loaded modified zeolite samples (P_i represents the inorganic fraction, P_o the organic fraction and P_r the residual fraction).

The sequential fractioning of the loaded modified zeolite revealed the existence of an important fraction of biological active phosphorus. Furthermore, the recovered phosphate can be suitable applied as fertilizer in P-deficient soils and finally it should be considered the abilities of the K-zeolites in soil improvement schemes. Cation exchange sites initially occupied by K cations are selectively exchanged with NH_4^+ and in less extension with Na^+, Ca^{2+} and Mg^{2+}. Then, they can be used as a slow acting fertilizer, mainly for K^+ and NH_4^+.

4. Conclusions

The modification of a powder natural zeolite into the potassium aluminium, iron and manganese forms allowed the simultaneous removal of ammonium and phosphate sorption from a secondary wastewater effluent. The sorption mechanisms identified were ion exchange in the case of ammonium and the formation of inner sphere complexes with the functional groups ≡M-OH (M: Al^{3+},

Fe^{3+}, Mn^{2+}) in the case of phosphate. Moreover, it was also found that electrostatic interactions occurred in both ammonium and phosphate sorption on modified zeolite. Particularly, the chemical precipitation of ammonium manganese hydrogen phosphate ($NH_4MnPO_4 \cdot H_2O$) was identified on the loaded modified potassium manganese zeolite. The maximum phosphate sorption capacity for the three zeolites were 6-80 mg-P/g for KALC, 7.2 mg-P/g for KFeC and to 8.2 mg-P/g for KMnC. Contrary ammonium maximum sorption capacity was constant between pH 4 and 9 for the tree zeolites as the main sorption mechanism is the ion-exchange involves the K^+ ions of the zeolite. The maximum ammonium sorption capacity for the three zeolites was approximately 29±3 mg-N/g.

The existence of organic matter content in treated wastewater not represented interference on the ammonium and phosphate sorption capacities for the three modified zeolite. The sequential fractioning of the loaded modified zeolite revealed on one hand the existence of an important fraction of biological active phosphorus and on the other hand that recovered phosphate is suitable as fertilizer in P-deficient soils. However, due to the limited reusability of these materials, it could be an interesting option as additives for the soil quality enhancement.

5. Acknowledgment

This study has been supported by the Waste2Product project (CTM2014-57302-R) financed by Ministry of Science and Innovation and the Catalan government (project ref. 2014SGR050). The authors gratefully acknowledge Dr. M. Hermassi (UPC) for research support, R. Estany (Aigues de Barcelona), M. Gullom (EMMA), I. Sancho (Centro Tecnologíco del Agua (CETaqua)). Zeocem (Slovakia) for zeolites supply. Finally, I. Lopez (Laboratory of Electronic Microscopy, Universitat Politècnica de Catalunya) for the FSEM analysis and to N. Moreno (IDAEA-CSIC) for XRD determinations. Diana Guaya acknowledges the financial support of Secretaría de Educación

Superior, Ciencia, Tecnología e Innovación (Senescyt - Ecuador) and Universidad Técnica Particular de Loja – Ecuador (Project - 2014: PROY_QUI_826).

6. References

[1] L. Lin, C. Wan, D.-J. Lee, Z. Lei, X. Liu, Ammonium assists orthophosphate removal from high-strength wastewaters by natural zeolite, Sep. Purif. Technol. 133 (2014) 351-356.

[2] A. Escudero, F. Blanco, A. Lacalle, M. Pinto, Struvite precipitation for ammonium removal from anaerobically treated effluents, J. Environ. Chem. Eng. 3 (2015) 413-419.

[3] SG. Lu, SQ. Bai, L. Zhu, HD. Shan, Removal mechanism of phosphate from aqueous solution by fly ash, J. Hazard Mater. 161 (2009) 95–101.

[4] O. Maaß, P. Grundmann, C. von Bock und Polach, Added-value from innovative value chains by establishing nutrient cycles via struvite, Resour. Conserv. Recy. 87 (2014) 126-136.

[5] G. Zelmanov, R. Semiat, The influence of competitive inorganic ions on phosphate removal from water by adsorption on iron (Fe3+) oxide/hydroxide nanoparticles-based agglomerates, J. Water Process Eng. 5 (2014) 143–152.

[6] H. Yin, M. Kong, Simultaneous removal of ammonium and phosphate from eutrophic waters using natural calcium-rich attapulgite-based versatile adsorbent, Desalination 351 (2014) 128-137.

[7] J. Xie, C. Li, L. Chi, D. Wu, Chitosan modified zeolite as a versatile adsorbent for the removal of different pollutants from water, Fuel 103 (2013) 480-485.

[8] J. Xie, W. Meng, D. Wu, Z. Zhang, H. Kong, Removal of organic pollutants by surfactant modified zeolite: Comparison between ionizable phenolic compounds and non-ionizable organic compounds, J. Hazard. Mater. 231–232 (2012) 57-63.

[9] X. Ji, M. Zhang, Y. Wang, Y. Song, Y. Ke, Y. Wang, Immobilization of ammonium and phosphate in aqueous solution by zeolites synthesized from fly ashes with different compositions, J. Ind. Eng. Chem. 22 (2015) 1-7.

[10] K. Margeta, N.Z. Logar, M. Šiljeg, A. Farkaš, Natural Zeolites in Water Treatment – How Effective is Their Use, 2013.

[11] H. Figueiredo, C. Quintelas, Tailored zeolites for the removal of metal oxyanions: Overcoming intrinsic limitations of zeolites, J. Hazard. Mater. 274 (2014) 287-299.

[12] D. Guaya, C. Valderrama, A. Farran, C. Armijos, J.L. Cortina, Simultaneous phosphate and ammonium removal from aqueous solution by a hydrated aluminum oxide modified natural zeolite, Chem. Eng. J. 271 (2015) 204-213.

[13] D. Guaya, C. Valderrama, A. Farran, J.L. Cortina, Modification of a natural zeolite with Fe(III) for simultaneous phosphate and ammonium removal from aqueous solutions, J. Chem. Technol. Biot. (2015) n/a-n/a.

[14] M.E. Villanueva, A. Salinas, G.J. Copello, L.E. Díaz, Point of zero charge as a factor to control biofilm formation of Pseudomonas aeruginosa in sol-gel derivatized aluminum alloy plates, Surf. Coat. Technol. 254 (2014) 145-150.

[15] A. APHA, WEF., Standard methods for the examination of water and wastewater, American Public Health Association, American Water Works Association, and Water Environment Federation, 2000.

[16] M.J. Hedley, J.W.B. Stewart, B.S. Chauhan, Changes in Inorganic and Organic Soil Phosphorus Fractions Induced by Cultivation Practices and by Laboratory Incubations, Soil. Sci. Soc. Am. J. 46 (1982) 970-976.

[17] J. Murphy, J.P. Riley, A modified single solution method for the determination of phosphate in natural waters, Anal. Chim. Acta. 27 (1962) 31-36.

[18] M.A. Malik, P. Marschner, K.S. Khan, Addition of organic and inorganic P sources to soil – Effects on P pools and microorganisms, Soil. Biol. Biochem. 49 (2012) 106-113.

[19] D.B. Abdala, I.R. da Silva, L. Vergütz, D.L. Sparks, Long-term manure application effects on phosphorus speciation, kinetics and distribution in highly weathered agricultural soils, Chemosphere 119 (2015) 504-514.

[20] C. Valderrama, J.I. Barios, M. Caetano, A. Farran, J.L. Cortina, Kinetic evaluation of phenol/aniline mixtures adsorption from aqueous solutions onto activated carbon and hypercrosslinked polymeric resin (MN200), React. Funct. Polym. 70 (2010) 142-150.

[21] G. Moussavi, S. Talebi, M. Farrokhi, R.M. Sabouti, The investigation of mechanism, kinetic and isotherm of ammonia and humic acid co-adsorption onto natural zeolite, Chem. Eng. J. 171 (2011) 1159-1169.

[22] F. Benaliouche, Y. Boucheffa, F. Thibault-Starzyk, In situ FTIR studies of propene adsorption over Ag- and Cu-exchanged Y zeolites, Micropor. Mesopor. Mat. 147 (2012) 10-16.

[23] T.C. Nguyen, P. Loganathan, T.V. Nguyen, S. Vigneswaran, J. Kandasamy, R. Naidu, Simultaneous adsorption of Cd, Cr, Cu, Pb, and Zn by an iron-coated Australian zeolite in batch and fixed-bed column studies, Chem. Eng. J. 270 (2015) 393-404.

[24] W. Zhang, X. Xiao, L. Zheng, C. Wan, Fabrication of TiO2/MoS2@zeolite photocatalyst and its photocatalytic activity for degradation of methyl orange under visible light, Appl. Surf. Sci.

[25] K. Chakarova, P. Nikolov, K. Hadjiivanov, Different Brønsted acidity of H-ZSM-5 and D-ZSM-5 zeolites revealed by the FTIR spectra of adsorbed CD3CN, Catal Commun. 41 (2013) 38-40.

[26] K. Góra-Marek, K. Brylewska, K.A. Tarach, M. Rutkowska, M. Jabłońska, M. Choi, L. Chmielarz, IR studies of Fe modified ZSM-5 zeolites of diverse mesopore topologies in the terms of their catalytic performance in NH3-SCR and NH3-SCO processes, Appl. Catal. B-Environ. 179 (2015) 589-598.

[27] O.B. Ayodele, H.U. Farouk, J. Mohammed, Y. Uemura, W.M.A.W. Daud, Hydrodeoxygenation of oleic acid into n- and iso-paraffin biofuel using zeolite supported fluoro-oxalate modified molybdenum catalyst: Kinetics study, J. Taiwan. Inst. Chem. E. 50 (2015) 142-152.

[28] A. Dhillon, M. Nair, S.K. Bhargava, D. Kumar, Excellent fluoride decontamination and antibacterial efficacy of Fe–Ca–Zr hybrid metal oxide nanomaterial, J. Colloid. Interf. Sci. 457 (2015) 289-297.

[29] K. Rida, S. Bouraoui, S. Hadnine, Adsorption of methylene blue from aqueous solution by kaolin and zeolite, Appl. Clay. Sci. 83–84 (2013) 99-105.

[30] F. Qi, B. Xu, Z. Chen, J. Ma, D. Sun, L. Zhang, Influence of aluminum oxides surface properties on catalyzed ozonation of 2,4,6-trichloroanisole, Sep. Purif. Technol. 66 (2009) 405-410.

[31] E.B. Simsek, E. Özdemir, U. Beker, Zeolite supported mono- and bimetallic oxides: Promising adsorbents for removal of As(V) in aqueous solutions, Chem. Eng. J. 220 (2013) 402-411.

[32] L.-C. Wang, Q. Liu, X.-S. Huang, Y.-M. Liu, Y. Cao, K.-N. Fan, Gold nanoparticles supported on manganese oxides for low-temperature CO oxidation, Appl. Catal. B-Environ. 88 (2009) 204-212.

[33] E. Ortega-Gómez, B. Esteban García, M.M. Ballesteros Martín, P. Fernández Ibáñez, J.A. Sánchez Pérez, Inactivation of natural enteric bacteria in real municipal wastewater by solar photo-Fenton at neutral pH, Water. Res. 63 (2014) 316-324.

[34] N. Murayama, M. Tanabe, H. Yamamoto, J. Shibata, Reaction, Mechanism and Application of Various Zeolite Syntheses from Coal Fly Ash, Mater. Trans. 44 (2003) 2475-2480.

[35] A. Malovanyy, H. Sakalova, Y. Yatchyshyn, E. Plaza, M. Malovanyy, Concentration of ammonium from municipal wastewater using ion exchange process, Desalination 329 (2013) 93-102.

[36] G.M. Walker, L.R. Weatherley, Kinetics of acid dye adsorption on GAC, Water. Res. 33 (1999) 1895-1899.

[37] M.S. Onyango, D. Kuchar, M. Kubota, H. Matsuda, Adsorptive Removal of Phosphate Ions from Aqueous Solution Using Synthetic Zeolite, Ind. Eng. Chem. Res. 46 (2007) 894-900.

[38] C. Li, S. Wu, R. Dong, Dynamics of organic matter, nitrogen and phosphorus removal and their interactions in a tidal operated constructed wetland, J. Environ. Manage. 151 (2015) 310-316.

[39] H. Huang, D. Xiao, R. Pang, C. Han, L. Ding, Simultaneous removal of nutrients from simulated swine wastewater by adsorption of modified zeolite combined with struvite crystallization, Chem. Eng. J. 256 (2014) 431-438.

Supplementary Material

Click here to download Supplementary Material: Supplementary material_JECE.docx